New BIOTECHNOLOGY 66 (2022) 89–96

Contents lists available at ScienceDirect

New BIOTECHNOLOGY

journal homepage: www.elsevier.com/locate/nbt

Full length Article

Phenoplate: An innovative method for assessing interacting effects of temperature and light on non-photochemical quenching in microalgae under chemical stress

Andrei Herdean *, Donna L. Sutherland, Peter J. Ralph

University of Technology Sydney, Climate Change Cluster, Ultimo, NSW, 2007, Australia

ARTICLE INFO

Keywords:
Phenoplate
Phenotyping
Photobiology
Temperature gradient
Rapid light curve
NPQ

ABSTRACT

Rapid light curves are one of the most widely used methods for assessing the physiological state of photosynthetic organisms. While the method has been applied in a range of physiological studies over the last 20 years, little progress has been made in adapting it for the new age of multi-parametric phenotyping. In order to advance research that is aimed at evaluating the physiological impact of multiple factors, the Phenoplate was developed: a simultaneous assessment of temperature and light gradients. It was used to measure rapid light curves of three marine microalgae across a temperature gradient and altered phosphate availability. The results revealed that activation of photoprotective mechanisms occurred with high efficiency at lower temperatures, and relaxation of photoprotection was negatively impacted above a certain temperature threshold in *Tetraselmis* sp. It was observed that *Thalassiosira pseudonana* and *Nannochloropsis oceanica* exhibited two unique delayed non-photochemical quenching signatures: in combinations of low light with low temperature, and darkness with high temperature, respectively. These findings demonstrate that the Phenoplate approach can be used as a rapid and simple tool to gain insight into the photobiology of microalgae.

Introduction

Methods based on variable chlorophyll *a* fluorescence for assessment of physiological status in photosynthetic organisms have been the preferred techniques for over 50 years of research in plant and microalgal studies [1] The measurement directly probes the photosynthetic machinery of the cell, specifically Photosystem II (PSII), as well as Photosystem I (PSI) to a certain extent [2]. The results can be used to understand the organism's physiology beyond the photosynthetic machinery, as most biological pathways, directly or indirectly, depend on photosynthesis. Over the years, a plethora of chlorophyll *a* fluorescence methods have been developed for a range of applications, for example simple flash induced fluorescence [3], pulse amplitude modulated fluorescence (PAM) [4], high-resolution fast fluorescence induction [5, 6], fast repetitive rate fluorescence (fRRF) [7], and terrestrial fluorescence observations from satellites [8]. The instruments used were initially built by the researchers themselves, but gradually commercial versions became available. One such instrument is the WALZ Imaging PAM [9], which measures chlorophyll *a* fluorescence *via* a charged-couple device (CCD) camera. Other commercial [10] and custom built instruments [11] that perform similar measurements are also available. The advantage provided by the imaging system is that multiple samples, or multiple areas of larger photosynthetic organisms, can be measured simultaneously and sample heterogeneity can be easily evaluated.

Understanding the interactive effects of multiple stressors, such as temperature, light, nutrients, pH and CO_2 on the physiological performance of photosynthetic organisms is fundamental to predicting responses to climate change [12]. Assessments of interacting effects of such multiple stressors have traditionally been laborious and time consuming. Here, an experimental protocol is demonstrated for performing high-throughput photo-physiological measurements along multiple stressor gradients, simultaneously. This was achieved by combining the Imaging PAM with a widely available laboratory

Abbreviations: PSI, Photosystem I; PSII, Photosystem II; PAM, pulse amplitude modulated fluorescence; fRRF, fast repetitive rate fluorescence; Y(II), quantum yield of PSII; Y(NPQ), quantum yield of regulated non-photochemical quenching of energy loss in PSII; Y(NO), quantum yield of non-regulated energy loss in PSII; rETR, relative electron transfer rates; NPQ, non-photochemical quenching; CBB, Calvin–Benson–Bassham; RLC, rapid light curve; qE, energy dependent component of NPQ.

* Corresponding author at: PO Box 123, Broadway, NSW, 2007, Australia.
E-mail addresses: andrei.herdean@uts.edu.au (A. Herdean), Donna.Sutherland@uts.edu.au (D.L. Sutherland), peter.ralph@uts.edu.au (P.J. Ralph).

https://doi.org/10.1016/j.nbt.2021.10.004
Received 13 May 2021; Received in revised form 21 October 2021; Accepted 23 October 2021
Available online 29 October 2021

thermocycler, used in polymerase chain reaction (PCR) experiments. The experiment was designed to study the short-term response of microalgae to the interacting effects of multiple environmental stressors, and thus revealing a part of its phenotype. The phosphorus (P) content in different samples was altered with the aim of limiting its availability to the thylakoid membrane ATP synthase to observe how this limitation impacts the photosynthetic response to various temperatures. Phenomics is an emerging discipline in algal research and will yield widespread impact across a range of biotechnology applications; however, developing tools to rapidly screen multiple strains/species/mutants across a range of conditions remains a technology constraint [13]. The Phenoplate will make a contribution to the development of this discipline. The experimental procedure has been termed the Phenoplate Analysis.

Materials and methods

Cell culture conditions

Cultures of the marine microalgal species *Tetraselmis* sp. (CS-91), *Thalassiosira pseudonana* (CS-173), and *Nannochloropsis oceanica* (CS-179) were obtained from the Commonwealth Scientific and Industrial Research Organisation (CSIRO; Canberra, ACT, Australia) culture collection. All three species belong to different phyla. *Tetraselmis* sp. belongs to Chlorophyta (or green algae), and contains the photosynthetic pigments chlorophyll *a* and *b*. *T. pseudonana* belongs to Bacillariophyta (diatoms) and contains chlorophylls *a* and *c*, together with the accessory pigments beta-carotene, fucoxanthin, diatoxanthin and diadinoxanthin. *N. oceanica* belongs to the phylum Ochrophyta, and contains chlorophyll *a*, as well as the accessory pigments astaxanthin, zeaxanthin and canthaxanthin. Inoculum cultures were diluted with their respective media, to give an initial optical density (OD_{750}) of 0.08 for each culture. OD_{750} was measured with a Tecan Infinite M1000 PRO plate reader (Tecan Schweiz AG, Männedorf, Switzerland). All three species were grown in 70 ml Corning Falcon tissue culture flasks (REF 353108, Corning Incorporated, NY, USA), containing 50 ml of either standard F/2 marine culture media, containing 1.5 mg L^{-1} of phosphorus (P), F/2 with only 25 % P concentration (0.4 mg L^{-1}) of standard F/2, or F/2 with 200 % P concentration (3.0 mg L^{-1}) of standard F/2. The F/2 media was made according to the recipes in [14] and [15]. The flasks were placed on a shaker table (TS-620, Thermoline Scientific, Fairfield, NSW, Australia) at 80 rpm, and cultures were grown under 70 µmol photons m^{-2} s^{-1} of cool white light provided by a Hydra LED lamp (Aqua Illumination, Allentown, PA, USA), on a 16:8 h light:dark cycle, at 20 °C, until late exponential growth was reached (2 weeks). After the two-week period in F/2, cells were harvested by centrifugation and transferred to new media (described above), while one set of F/2 cultures was transferred to P-free F/2, and all cultures maintained under the same growth conditions for a further week. At the end of the culture period, the OD_{750} measurements for 25 % P, standard F/2 and 200 % P treatments were 0.70, 0.79, and 0.85 for *N. oceanica*, 0.26, 0.32 and 0.28 *Tetraselmis* sp. and 0.74, 0.82 and 0.84 for *T. pseudonana.* One tissue culture flask was cultured for each condition and each species tested. Each flask was sampled 4 times for the Phenoplate measurements.

Imaging PAM measurement

Fluorescence measurements were performed using a MAXI PAM Imaging system, model IMAG-MAX/L (Walz, Effeltrich, Germany). The system is fitted with a 12.5 mm f/1:1.4 Pentax TV Lens attached to a Walz digital interface model IMAG-MAX/K. Before measurements, the lens was focused on the sample using the focusing ring with the infra-red LEDs turned on so that the image was clearly visible on the screen. Actinic light and saturation pulses were provided by a blue LED array with a peak wavelength at 450 nm. A customised measurement protocol was used, which consisted of 30 min dark adaptation and temperature acclimation, followed by a rapid light curve (RLC), transition to low light, and then dark recovery. The light protocol was as follows: 11 (10 s), 21 (10 s), 36 (10 s), 56 (10 s), 81 (10 s), 111 (10 s), 146 (10 s), 186 (10 s), 231 (10 s), 11 (80 s), 0 (180 s) µmol photons m^{-2} s^{-1}.

Phenoplate measurement

The Phenoplate consisted of a relatively simple combination of two instruments, each with their own custom protocol. The protocol used to assess the physiological status consisted of three consecutive sequences that were designed to probe: (i) the response to increasing light intensity (rapid light curve), (ii) the transition to low light, and (iii) the dark relaxation or recovery (Fig. 1A). Each sequence of the protocol was designed to address different photosynthetic response mechanisms. At the same time, the influence of various temperatures on these mechanisms was investigated using a relatively short temperature treatment of the samples using a thermocycler (Fig. 1C). Each probing saturation pulse of the Imaging PAM was used to generate composite images of calculated photosynthetic parameters such as quantum yield of PSII (Y(II)), quantum yield of regulated non-photochemical quenching of energy loss in PSII (Y(NPQ)), and quantum yield of non-regulated energy loss in PSII (Y(NO)) (Fig. 1D). This data, together with the measured light intensity, was used by the Imaging PAM software (Walz, Effeltrich, Germany) to calculate the relative electron transfer rates (rETR) and the non-photochemical quenching (NPQ).

For high-throughput measurements of each species, 200 µl of culture was added in each well of a PCR 96 microwell plate (HSP9655, Bio-Rad Laboratories, Inc, Hercules, CA, USA). The microwell plates were placed on the sample block of the thermocycler (ABI Veriti, Applied Biosystems, Waltham, MA, USA), while the Imaging PAM was positioned over the plate to keep the sample in darkness during the 30 min dark-adaptation and temperature treatment. The thermocycler was programmed to generate and hold a temperature gradient for every pair of columns of the plate, ranging from 10 to 35 °C (Fig. 1B). The PAM measurement was initiated at the end of the 30 min incubation period. The temperature range was chosen so as to provide an upper and lower deviation of at least 10 °C from the optimal growth temperature of the microalgae, which ranges between 19-21 °C [16,17].

Statistical analyses

Statistical analyses were performed using either analysis of variance (ANOVA) for comparison between treatments, or principal component analysis (PCA) for assessment of effects across the treatment matrix. For ANOVA, if a main effect was significant, the ANOVA was followed by a Tukey's HSD test at significance $p < 0.05$ and $p < 0.01$. All statistical analyses were carried out using Statistica software (Statsoft Inc., Tulsa, OK, USA) and OriginPro (OriginLab Corp., Northampton, MA, USA).

Results

Data generated by the rapid light curve were used to create surface plots to visualise the relationship between temperature and rETR under P-replete conditions. For all three microalgal species, the highest rETR measured was observed at 30 °C, for at least one light intensity, but this light intensity varied between the species (36 µmol photons m^{-2} s^{-1} for *Tetraselmis* sp., 36 µmol photons m^{-2} s^{-1} for *T. pseudonana*, and 56 µmol photons m^{-2} s^{-1}. *N. oceanica*) (Fig. 2A-C, Supplementary Table 1). At low light intensity, rETR increased with increasing temperature, with rETR at 10 °C significantly lower ($p < 0.01$) than at 25 and 30 °C for *Tetraselmis* sp., although this trend was absent in the other two species (Fig. 2A-C, Supplementary Table 1A, B). Statistical analysis of each rETR matrix and raw data values are shown in Supplementary Table 1A, B.

For the interacting effects of P availability and temperature, the rETR matrix showed that both deplete (25 % P) and excess P (200 % P) concentrations resulted in decreased rETR, relative to the control P

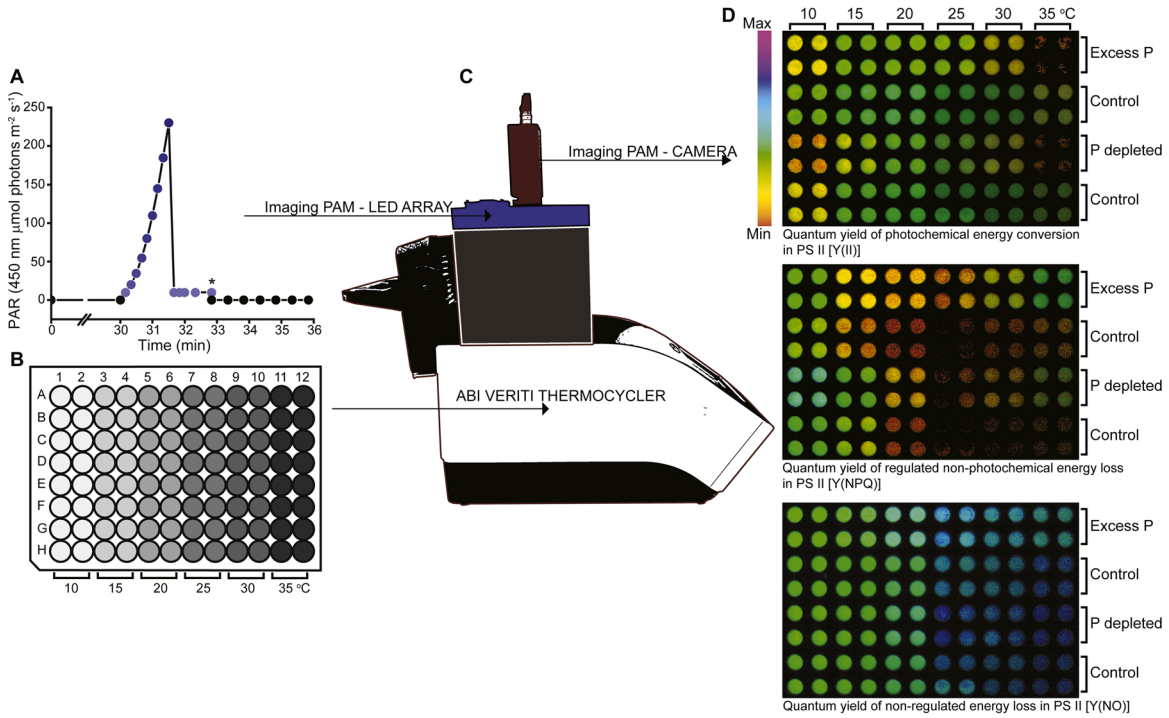

Fig. 1. The Phenoplate setup and example data. (A) Visual representation of the light exposure protocol of the Imaging PAM. "*" indicates the time point that is presented in part D of this figure. The vertical axis shows the intensity of the photosynthetic active radiation (PAR). (B) Temperature layout of 96 well plate containing the imaged samples. (C) visual representation of the complete Phenoplate setup which consists of the ABI Veriti thermocycler and the Walz Imaging PAM. (D) Example results extracted from the last time point of the transition to low light (marked with "*" in section A). Data shown is the microalga *Nannochloropsis oceanica* grown in standard F/2 media (Control), or F/2 media with excess phosphate (200 % P), or media depleted of phosphate (25 % P), relative to F/2.

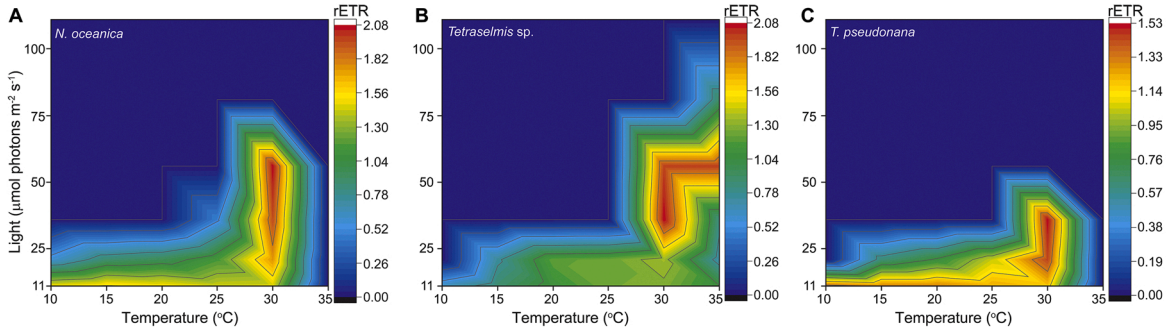

Fig. 2. Relative Electron Transfer Rate of Photosystem II at different temperatures. Cultures of *Nannochloropsis oceanica* (A), *Tetraselmis* sp. (B), and *Thalassiosira pseudonana* (C) grown for 3 weeks in standard F/2 media were measured using the Phenoplate. No rETR was observed at higher light intensity due to strong development of NPQ (Fig. 5) or closure of PSII reaction centers. Data represents average of 4 measurements (n = 4).

(replete P) (Fig. 3A-C). PCA analysis of the 3 data sets indicate that the temperature/rETR matrix of the reduced P treatment was the most affected, whereas the matrix of the control and excess P were similar, despite the reduction in amplitude of rETR for the excess treatment (Fig. 3D). Statistical analysis of data points of each rETR matrix and raw data values are shown in Supplementary Table 2A-C.

The PAM protocol was designed to measure both NPQ induction and relaxation, thus providing a broader overview of the photoprotective process. The Imaging PAM was used to collect 20 composite images of the 96 well plate (Fig. 4A) which were transformed into classical plots for visualizing NPQ kinetics (Fig. 4B), while a 2D heat map provided a better visual representation of the complex data set (Fig. 4C). The results showed that NPQ became induced quickly at lower temperatures, while the mechanisms of relaxation under low light became inhibited at the lowest temperature in *Tetraselmis,* regardless of P treatment (Fig. 4 B,C). Nonetheless, changes in P availability did affect NPQ, with increased NPQ occurring in the P deplete treatment and decreased NPQ under excess P treatment (Fig. 4C). The NPQ induction and relaxation kinetics changed towards lower maximum and fast saturation in temperatures >20 °C, and higher maximum at temperatures <20 °C (Fig. 4B-C). The low NPQ at higher temperatures correlated well with the rETR which reached its maximum at 30 °C (Fig. 2B), which indicates that more

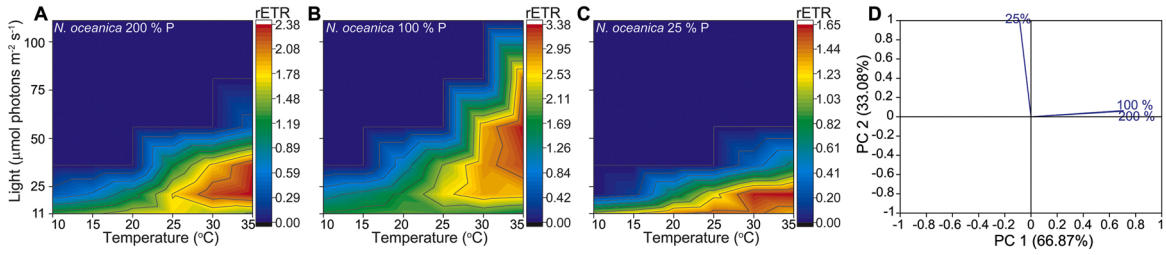

Fig. 3. Relative Electron Transfer Rate of Photosystem II at different temperatures and phosphate availability in *Nannochloropsis oceanica*. Cultures were grown in (A) media with excess phosphate (200 % P relative to F/2), (B) standard F/2 media, and (C) media depleted of phosphate (25 % P relative to F/2) for 2 weeks and transferred to media with no available phosphate for 1 week prior to the measurement as described in Materials and Methods. (D) PCA loading plot of the 3 rETR matrixes. No rETR was observed at higher light intensity due to strong development of NPQ (Fig. 5) or closure of PSII reaction centers. Data represents average of 4 measurements (n = 4).

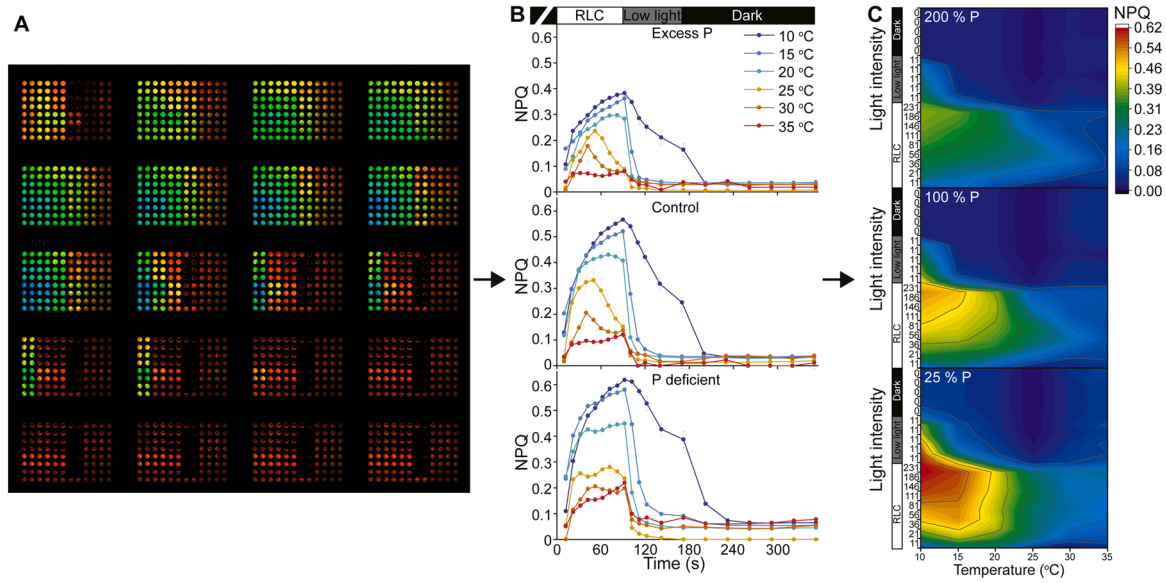

Fig. 4. NPQ data transformation of *Tetraselmis* sp. grown under varied phosphorus conditions. (A) Image data from the Imaging PAM. Each one of the 20 groups of dots represent one processed image showing NPQ values from each saturation pulse during the measurement. The averaged values are shown in (B) along with the light exposure protocol at the top of the figure; white bar indicates exposure to increasing light intensities of the RLC, grey indicates low light, and black indicates darkness. C) 2D heat map plots of the corresponding NPQ data from section B.

energy can be collected and directed towards photochemistry at higher temperatures. This observation can be explained by activation of the Calvin–Benson–Bassham (CBB) cycle by rubisco activase for which the optimum working temperature is 30 °C [18].

Unlike the NPQ surface plots of *Tetraselmis* sp. (Figs. 4C, 5 D-F), the NPQ surface plots of *T. pseudonana* and *N. oceanica* revealed unexpected responses, in addition to showing elevated NPQ (Fig. 5A-C, G-I). Different temperature and light combinations generated three distinct NPQ components, which were seen in almost all measurements, but were best observed under phosphate limitation (Fig. 5C, I). These different components were the following. (i) A high NPQ response to high light, probably driven by energy dependent quenching (qE) [19, 20], which appeared between 186 and 231 µmol photons m^{-2} s^{-1}, at the end of the RLC and between 20 and 35 °C; this component was clearly distinguishable in Fig. 5C, I and Supplementary Fig. 1A, C, G, H, I, but weakly visible in Fig. 5B and Supplementary Fig. 1B (*N. oceanica* in F/2 media); (ii) A delayed low light NPQ response visible after ~1 min exposure to low light (11 µmol photons m^{-2} s^{-1}), which was only detected at 10 and 15 °C; (iii) A delayed NPQ that appeared only at 35 °C in the final measurement points, during the dark relaxation (Fig. 5C, I; Supplementary Fig. 1 ABC-GHI).

Discussion

Temperature and light are fundamentally connected in modulation of cell metabolism. The way these abiotic factors influence microalgae are species specific. The Phenoplate approach offers an easy and rapid way of assessing how these factors interact, along defined gradients, to understand the cell's photobiology. The Phenoplate offers the possibility of adding a third stressor, such as a nutrient or a toxicant, to the assessment. Various Phenoplate-like measurements can be found in the literature [21] but none as comprehensive, nor in the currently presented form. The closest approach to the Phenoplate is the PhenoChip which uses a similar temperature and imaging approach, but is aimed at single cell studies, and uses proprietary equipment not yet available to the wider community [22]. The Phenoplate can be used with almost any

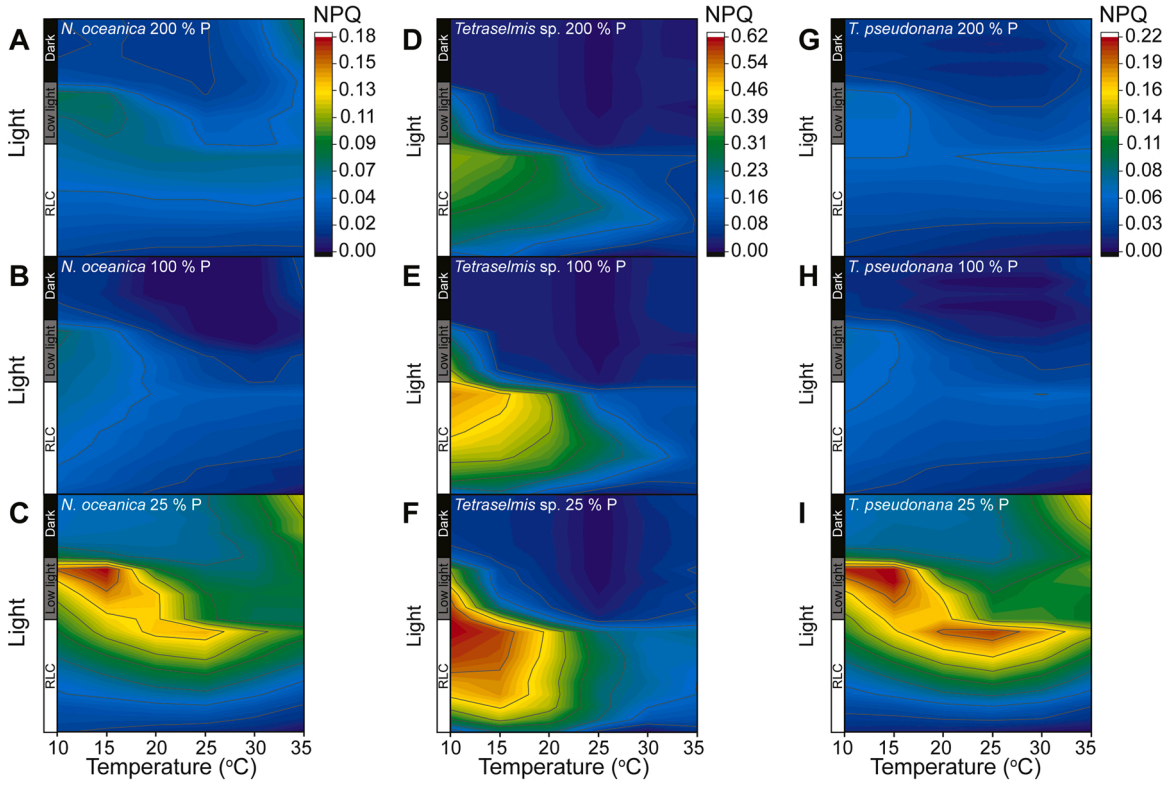

Fig. 5. NPQ surface plots of, *Nannochloropsis oceanica*, *Tetraselmis* sp., *and Thalassiosira pseudonana*. Two weeks old cultures grown with different phosphorus (P) availability were measured with the Phenoplate. A, B and C represent measurements of *N. oceanica* grown in (A) 200 % P concentration (of F/2 media), (B) 100 % P concentration, and (C) 25 % P concentration. Figures D, E and F are repeated from Fig. 4C and represent measurements of *Tetraselmis* sp. grown in (D) 200 % P concentration (of F/2 media), (E) 100 % P concentration, and (E) 25 % P concentration. G, H and I represent measurements of *T. pseudonana* grown in (G) 200 % P concentration (of F/2 media), (H) 100 % P concentration, and (I) 25 % P concentration. Surface plots are scaled to maximum and minimum from all 3 treatments for each species. Individual scaled plots are shown in Supplementary Fig. 1. Data represents average of 4 measurements (n = 4).

thermocycler, allowing use of precisely timed temperature changes, temperature gradients and taking advantage of the medical grade temperature accuracy of the thermocycler. Traditionally, the effects of shifts in temperature regime on algal physiology have been investigated using temperature adapted cultures (multiple cell divisions) along temperature gradients [23–25], rather than on cultures temporarily exposed to temperature treatments. In the present study, the Phenoplate allowed the assessment of short-term photophysiological responses to changes in temperature (30 min) combined with additional stressors (in this case, light and phosphorus), using a set of widely available instruments.

The highest rETR recorded at temperatures up to 10 °C higher than the culture growth conditions, suggests that some constraining factor on the cell metabolism, or photosynthetic machinery, relaxed with increased temperature. The short duration of the temperature treatment was not expected to result in any substantial biological changes, thus suggesting that the constraining factor that relaxed during higher temperature treatments was physical in nature. One possibility is that under higher temperatures, an increase in membrane fluidity facilitates the diffusion processes between PSII and PSI [26], while an alternative is that elevated temperature facilitates changes in protein conformation required for photosynthesis, thereby removing some constraints on the electron transfer chain [27]. The addition of a P availability treatment demonstrated the utility of the Phenoplate to assess the effects of multiple stressors on photophysiology. While rETR was reduced under P deficiency, the overall pattern of the temperature/rETR landscape remained unaltered, suggesting that it reflects intrinsic properties of these organisms that are not expected to change, even after long-term adaptation to new abiotic conditions. Evidence suggests that the principal target of phosphate deficiency is a limitation on the activity of ATP synthase [28], which was probably the case in the microalgal strains we tested. It is interesting to note that the general patterns of temperature/rETR and NPQ/rETR were very similar between *N. oceanica* and *T. pseudonana*.

To date, few studies have looked in detail at the relationship between NPQ and temperature using gradients [29–31], and those that have were focused on thermal adaptation rather than short term thermal impacts. The advantage of a brief thermal change in the cell's environment is that the measurement determines temperature response rather than adaptation. NPQ is the sum of multiple mechanisms, which depend on the thylakoid membrane pH gradient [32,33], light harvesting antennae phosphorylation [34], membrane architecture [35], ion transporters [36,37], phosphate availability [28] and essential NPQ proteins (*e.g.* PsbS, LHCSR) [38,39]. The PAM measurement was designed here to probe mainly the energy dependent component (qE) of NPQ [19], as well as relaxation kinetics to low light and darkness [36]. The RLC part of the protocol was designed to activate the pH and ion transporter dependent NPQ mechanisms [40,20]. The protocol continued with transition to low light recovery conditions, which has been demonstrated to be a distinct process dependent on cation proton exchange [36], critical for conditions of fluctuating light. The final part of the measurement determines if there is any slowly reversible NPQ generated during the RLC.

The Phenoplate measurement revealed that in *Tetraselmis* sp., once a lower temperature threshold was reached (10 °C), NPQ relaxation to low light appeared to be severely impacted relative to higher temperatures. This type of impairment resembles measurements seen in *Arabidopsis*

thaliana mutants that have a thylakoid potassium proton antiporter knocked out [36,37]. If a similar process exists in *Tetraselmis* it may indicate that proteins responsible for this type of ion exchange have a specific range of temperature that they can tolerate. No other NPQ component appeared to be negatively impacted at 10 °C, and the cells generated a high NPQ which eventually completely relaxed in darkness, suggesting that low temperature targets a specific and limited number of processes required for dynamic adaptation to fluctuating light conditions.

Another interesting finding regarding the relationship between NPQ and temperature was that *T. pseudonana* and *N. oceanica* developed unique NPQ responses at different combinations of temperature and light. To the best knowledge of the authors, the low light (11 μmol photons m^{-2} s^{-1}) with low temperature (10 and 15 °C) NPQ response in *Tetraselmis* sp. has not been documented before. NPQ is known to occur in low light, but it is very unusual for it to exceed the amplitude of the NPQ in high light [41,42]. Furthermore, this type of NPQ appears to be fully reversible since it completely relaxed in darkness. A time-dependent buildup of ATP due to temperature inactivated CBB and a subsequent acidification of the thylakoid lumen could explain the result. Nonetheless, this finding merits further experimentation to elucidate the precise nature of the underlying process and any implications it may have in conditions of fluctuating temperature and light.

Lastly, signs of a delayed NPQ response were observed after the illumination steps that appeared at higher temperatures, 35 °C and potentially above. This can be seen at the edge of the temperature/NPQ matrix at highest temperature and final dark relaxation points. The fact that it developed in darkness suggests that temperature may be the main element driving this process, and it could be a mechanism similar to the super-quenching state observed in *Symbiodinium* [43]. The manganese cluster of the oxygen-evolving complex has also been shown to be particularly sensitive to high temperature which, in combination with light, could also generate the observed NPQ [44,45]. Migration of light harvesting antennae from PSII to PSI, also known as state transition to State 2 [46], as well as enhanced chlororespiration [47] induced by elevated temperature [48] can result in an apparent increase in NPQ in the dark.

Limitations

There is experimental evidence from plant research showing that there is a lag phase in the activation kinetics of the CBB cycle as well as a temperature dependence of the activation rate [49]. Furthermore, *in vitro* research has shown that ribulose-1,5-bisphosphate carboxylase-oxygenase (RuBisCo) activity increases linearly with temperature and that the activity of rubisco activase follows closely, but stops working at elevated temperatures [18]. It is extremely difficult to determine with certainty if the temperature impact on the CBB cycle has a major effect on the results of the RLC and/or NPQ. Decoupling the effect of temperature on the CBB cycle and light harvesting can be accomplished *in vitro*, but that is beyond the scope of this research. Therefore, the impact of the CBB cycle on rETR and NPQ was not considered in interpretation of the results.

Different cell density, or total chlorophyll content per sample, can have an impact on chlorophyll *a* fluorescence measurements. The principal phenomenon that affects the measurement is light attenuation due to high cell density [50]. This is particularly problematic when multiple samples are measured simultaneously using a PAM imaging system. Samples with large differences in cell density are almost impossible to measure at the same time since the camera sensitivity needs to be adjusted for each sample to avoid over- or under-exposure of the camera. To avoid such problems sample density can be adjusted prior to measurements. In the present work this was not possible since it would have resulted in an additional change in P content in the media. Nonetheless, an almost 10-fold difference in chlorophyll concentrations of algal suspensions have been documented to result in less than 5% variability using a similar imaging system [51].

To avoid any misinterpretation that could have resulted from the possible effect of different sample concentration, direct comparisons between different phosphate treatments were minimized and instead conclusions were drawn from the general patterns that emerged from each treatment. Exceptions to this are instances were raw data from the Phenoplate was presented and where statistical analysis was performed on all samples.

Application

This investigation has demonstrated how the Phenoplate can provide high-throughput assessment of multiple stressors on the photophysiology of microalgae, under short-term incubations (30 min). This technique could allow for the assessment of multiple stressor effects on wild populations of microalgae without the complication of adaptation to laboratory conditions that longer-term incubations would create. High-throughput assessment of multiple stressors, using the Phenoplate, could also be applied to toxicology studies to assess acute effects and interactions. Currently, such studies involve using a limited range of test species, grown under standardised light and temperature conditions and exposure to one toxicant [52]. These conditions are not representative of the changing environment in nature and the interactive effect of variable light and temperature on the toxicant are missed. Improved methodologies for multi-stressor assessments, such as the Phenoplate, will help improve our knowledge on these interacting effects for improved environmental outcomes.

Conclusions

In the present research, the Phenoplate was used to reveal multiple unique NPQ responses that have not been previously documented, each appearing at precise phosphate, temperature and light combinations. These findings are in agreement with a previously documented NPQ response to phosphate starvation [53] and the NPQ response to various temperatures [54]. The findings will form the basis of additional projects aimed to elucidate the nature of the mechanisms involved. To meet the requirements of the emerging field of algal phenotyping, the Phenoplate method upgrades the classic rapid light curve measurement that has remained unchanged for over 20 years [55]. The use of a thermocycler together with the Imaging PAM make multiparametric measurements easily available and opens up a multitude of new types of experiments. Future work using this system could expand the temperature range used to anywhere between 0 °C and 100 °C, the PAM protocol can also be altered to answer specific questions, and the measurement could be extended to measure 384 samples simultaneously. Furthermore, the Phenoplate measurement has important implications for research in microalgae ecology and biotechnology, where fast and sensitive measurement methods are needed to gain insights into the interactive effects of multiple stressors on the organism.

Author contributions

Andrei Herdean: conceptualization, methodology, validation, investigation, writing - original draft, visualization. Donna Sutherland: validation, investigation, resources, writing - review & editing. Peter Ralph: writing - review & editing, supervision, funding acquisition, resources.

Declarations of interest: none

Declaration of Competing Interest

The authors declare that they have no known competing financial interests or personal relationships that could have appeared to influence the work reported in this paper.

Appendix A. Supplementary data

Supplementary material related to this article can be found, in the online version, at doi:https://doi.org/10.1016/j.nbt.2021.10.004.

References

[1] Vredenberg WJ, Slooten L. Chlorophyll *a* fluorescence and photochemical activities of chloroplast fragments. Biochim Biophys Acta 1967;143:583–94. https://doi.org/10.1016/0005-2728(67)90064-3.

[2] Schreiber U, Klughammer C. Evidence for variable chlorophyll fluorescence of photosystem I in vivo. Photosynthesis Res 2021. https://doi.org/10.1007/s11120-020-00814-y.

[3] Genty B, Briantais J-M, Baker NR. The relationship between the quantum yield of photosynthetic electron transport and quenching of chlorophyll fluorescence. Biochim Biophys Acta Gen Subj 1989;990:87–92. https://doi.org/10.1016/s0304-4165(89)80016-9.

[4] Schreiber U, Endo T, Mi H, Asada K. Quenching analysis of chlorophyll fluorescence by the saturation pulse method: particular aspects relating to the study of eukaryotic algae and cyanobacteria. Plant Cell Physiol 1995;36:873–82. https://doi.org/10.1093/oxfordjournals.pcp.a078833.

[5] Bates H, Zavafer A, Szabó M, Ralph PJ. A guide to Open-JIP, a low-cost open-source chlorophyll fluorometer. Photosynthesis Res 2019;142:361–8. https://doi.org/10.1007/s11120-019-00673-2.

[6] Strasser RJ. The Fo and the OJIP fluorescence rise in higher plants and algae. Aghia Pelaghia. Springer; 1992.

[7] Kolber ZS, Prášil O, Falkowski PG. Measurements of variable chlorophyll fluorescence using fast repetition rate techniques: defining methodology and experimental protocols. Biochim Biophys Acta 1998;1367:88–106. https://doi.org/10.1016/S0005-2728(98)00135-2.

[8] Joiner J, Yoshida Y, Vasilkov AP, Yoshida Y, Corp LA, Middleton EM. First observations of global and seasonal terrestrial chlorophyll fluorescence from space. Biogeosciences 2011;8:637–51. https://doi.org/10.5194/bg-8-637-2011.

[9] Hill R, Schreiber U, Gademann R, Larkum AWD, Kühl M, Ralph PJ. Spatial heterogeneity of photosynthesis and the effect of temperature-induced bleaching conditions in three species of corals. Mar Biol 2004;144:633–40. https://doi.org/10.1007/s00227-003-1226-1.

[10] Nedbal L, Soukupová J, Kaftan D, Whitmarsh J, Trtílek M. Kinetic imaging of chlorophyll fluorescence using modulated light. Photosynthesis Res 2000;66:3–12. https://doi.org/10.1023/A:1010729821876.

[11] Cruz JA, Savage LJ, Zegarac R, Hall CC, Satoh-Cruz M, Davis GA, et al. Dynamic environmental photosynthetic imaging reveals emergent phenotypes. Cell Syst 2016;2:365–77. https://doi.org/10.1016/j.cels.2016.06.001.

[12] Yong W-K, Sim K-S, Poong S-W, Wei D, Phang S-M, Lim P-E. Interactive effects of temperature and copper toxicity on photosynthetic efficiency and metabolic plasticity in Scenedesmus quadricauda (Chlorophyceae). J Appl Phycol 2018;30:3029–41. https://doi.org/10.1007/s10811-018-1574-3.

[13] Fabris M, Abbriano RM, Pernice M, Sutherland DL, Commault AS, Hall CC, et al. Emerging technologies in algal biotechnology: toward the establishment of a sustainable, algae-based bioeconomy. Front Plant Sci 2020:11. https://doi.org/10.3389/fpls.2020.00279.

[14] Guillard RRL, Ryther JH. Studies of marine planktonic diatoms: I. Cyclotella nana hustedt, and detonula confervacea (cleve) Gran. Can J Microbiol 1962;8:229–39. https://doi.org/10.1139/m62-029.

[15] Guillard RRL. Culture of phytoplankton for feeding marine invertebrates. Boston, MA: Springer US; 1975. p. 29–60.

[16] Abu-Rezq TS, Al-Musallam L, Al-Shimmari J, Dias P. Optimum production conditions for different high-quality marine algae. Hydrobiologia 1999;403:97–107. https://doi.org/10.1023/A:1003725626504.

[17] Sheehan CE, Baker KG, Nielsen DA, Petrou K. Temperatures above thermal optimum reduce cell growth and silica production while increasing cell volume and protein content in the diatom Thalassiosira pseudonana. Hydrobiologia 2020;847:4233–48. https://doi.org/10.1007/s10750-020-04408-6.

[18] Crafts-Brandner SJ, Salvucci ME. Rubisco activase constrains the photosynthetic potential of leaves at high temperature and CO2. Proc Natl Acad Sci U S A 2000;97:13430–5. https://doi.org/10.1073/pnas.230451497.

[19] Horton P, Ruban A, Walters R. Regulation of light harvesting in green plants. Annu Rev Plant Biol 1996;47:655–84. https://doi.org/10.1146/annurev.arplant.47.1.655.

[20] Nilkens M, Kress E, Lambrev P, Miloslavina Y, Müller M, Holzwarth AR, et al. Identification of a slowly inducible zeaxanthin-dependent component of non-photochemical quenching of chlorophyll fluorescence generated under steady-state conditions in Arabidopsis. Biochim Biophys Acta 2010;1797:466–75. https://doi.org/10.1016/j.bbabio.2010.01.001.

[21] Bates H, Zavafer A, Szabó M, Ralph P. The Phenobottle, an open-source photobioreactor platform for environmental simulation. Algal Res 2020;52:102105. https://doi.org/10.1016/j.algal.2020.102105.

[22] Behrendt L, Salek MM, Trampe EL, Fernandez VI, Lee KS, Kühl M, et al. PhenoChip: a single-cell phenomic platform for high-throughput photophysiological analyses of microalgae. Sci Adv 2020;6:eabb2754. https://doi.org/10.1126/sciadv.abb2754.

[23] Baker KG, Robinson CM, Radford DT, McInnes AS, Evenhuis C, Doblin MA. Thermal performance curves of functional traits aid understanding of thermally induced changes in diatom-mediated biogeochemical fluxes. Front Mar Sci 2016:3. https://doi.org/10.3389/fmars.2016.00044.

[24] Murata N, Fork DC. Temperature dependence of chlorophyll *a* fluorescence in relation to the physical phase of membrane lipids algae and higher plants. Plant Physiol 1975;56:791–6. https://doi.org/10.1104/pp.56.6.791.

[25] Thrane J-E, Hessen DO, Andersen T. Plasticity in algal stoichiometry: experimental evidence of a temperature-induced shift in optimal supply N:P ratio. Limnol Oceanogr 2017;62:1346–54. https://doi.org/10.1002/lno.10500.

[26] Yamori W, Noguchi K, Kashino Y, Terashima I. The role of Electron transport in determining the temperature dependence of the photosynthetic rate in spinach leaves grown at contrasting temperatures. Plant Cell Physiol 2008;49:583–91. https://doi.org/10.1093/pcp/pcn030.

[27] Wang H, Lin S, Katilius E, Laser C, Allen JP, Williams JC, et al. Unusual temperature dependence of photosynthetic Electron transfer due to protein dynamics. J Phys Chem 2009;113:818–24. https://doi.org/10.1021/jp807468c.

[28] Carstensen A, Herdean A, Schmidt SB, Sharma A, Spetea C, Pribil M, et al. The impacts of phosphorus deficiency on the photosynthetic Electron transport chain. Plant Physiol 2018;177:271–84. https://doi.org/10.1104/pp.17.01624.

[29] Kulk G, de Vries P, van de Poll WH, Visser RJ, Buma AG. Temperature-dependent photoregulation in oceanic picophytoplankton during excessive irradiance exposure. Rijeka: IntechOpen 2013:209–28.

[30] Salvucci ME, Crafts-Brandner SJ. Relationship between the heat tolerance of photosynthesis and the thermal stability of rubisco activase in plants from contrasting thermal environments. Plant Physiol 2004;134:1460–70. https://doi.org/10.1104/pp.103.038323.

[31] Yin Y, Li S, Liao W, Lu Q, Wen X, CJJopp Lu. Photosystem II photochemistry, photoinhibition, and the xanthophyll cycle in heat-stressed rice leaves. J Plant Physiol 2010;167:959–66. https://doi.org/10.1016/j.jplph.2009.12.021.

[32] Briantais JM, Vernotte C, Picaud M, Krause GH. A quantitative study of the slow decline of chlorophyll a fluorescence in isolated chloroplasts. Biochim Biophys Acta 1979;548:128–38. https://doi.org/10.1016/0005-2728(79)90193-2.

[33] Tian L, Nawrocki WJ, Liu X, Polukhina I, Van Stokkum IH, Croce R. pH dependence, kinetics and light-harvesting regulation of nonphotochemical quenching in Chlamydomonas. Proc Natl Acad Sci U S A 2019;116:8320–5. https://doi.org/10.1073/pnas.1817796116.

[34] Bonente G, Ballottari M, Truong TB, Morosinotto T, Ahn TK, Fleming GR, et al. Analysis of LhcSR3, a protein essential for feedback de-excitation in the green alga Chlamydomonas reinhardtii. PLoS Biol 2011;9:e1000577. https://doi.org/10.1371/journal.pbio.1000577.

[35] Goss R, Oroszi S, Wilhelm C. The importance of grana stacking for xanthophyll cycle-dependent NPQ in the thylakoid membranes of higher plants. Physiol Plant 2007;131:496–507. https://doi.org/10.1111/j.1399-3054.2007.00964.x.

[36] Armbruster U, Carrillo LR, Venema K, Pavlovic L, Schmidtmann E, Kornfeld A, et al. Ion antiport accelerates photosynthetic acclimation in fluctuating light environments. Nat Commun 2014;5:1–8. https://doi.org/10.1038/ncomms6439.

[37] Dukic E, Herdean A, Cheregi O, Sharma A, Nziengui H, Dmitruk D, et al. K+ and Cl− channels/transporters independently fine-tune photosynthesis in plants. Sci Rep 2019;9:1–12. https://doi.org/10.1038/s41598-019-44972-z.

[38] Goss R, Lepetit B. Biodiversity of NPQ. J Plant Physiol 2015;172:13–32. https://doi.org/10.1016/j.jplph.2014.03.004.

[39] Tibiletti T, Auroy P, Peltier G, Caffarri S. Chlamydomonas reinhardtii PsbS protein is functional and accumulates rapidly and transiently under high light. Plant Physiol 2016;171:2717–30. https://doi.org/10.1104/pp.16.00572.

[40] Herdean A, Teardo E, Nilsson AK, Pfeil BE, Johansson ON, Ünnep R, et al. A voltage-dependent chloride channel fine-tunes photosynthesis in plants. Nat Commun 2016;7:1–11. https://doi.org/10.1038/ncomms11654.

[41] Dong Y-L, Jiang T, Xia W, Dong H-P, Lu S-H, Cui L. Light harvesting proteins regulate non-photochemical fluorescence quenching in the marine diatom Thalassiosira pseudonana. Algal Res 2015;12:300–7. https://doi.org/10.1016/j.algal.2015.09.016.

[42] Szabó M, Parker K, Guruprasad S, Kuzhiumparambil U, Lilley RM, Tamburic B, et al. Photosynthetic acclimation of Nannochloropsis oculata investigated by multi-wavelength chlorophyll fluorescence analysis. Bioresour Technol 2014;167:521–9. https://doi.org/10.1016/j.biortech.2014.06.046.

[43] Slavov C, Schrameyer V, Reus M, Ralph PJ, Hill R, Büchel C, et al. "Super-quenching" state protects Symbiodinium from thermal stress—implications for coral bleaching. Biochim Biophys Acta 2016;1857:840–7. https://doi.org/10.1016/j.bbabio.2016.02.002.

[44] Murata N, Takahashi S, Nishiyama Y, Allakhverdiev SI. Photoinhibition of photosystem II under environmental stress. Biochim Biophys Acta 2007;1767:414–21. https://doi.org/10.1016/j.bbabio.2006.11.019.

[45] Nash D, Miyao M, Murata N. Heat inactivation of oxygen evolution in Photosystem II particles and its acceleration by chloride depletion and exogenous manganese. Biochim Biophys Acta 1985;807:127–33. https://doi.org/10.1016/0005-2728(85)90115-X.

[46] Erickson E, Wakao S, Niyogi KK. Light stress and photoprotection in Chlamydomonas reinhardtii. Plant J 2015;82:449–65. https://doi.org/10.1111/tpj.12825.

[47] Dijkman NA, Kroon BMA. Indications for chlororespiration in relation to light regime in the marine diatom Thalassiosira weissflogii. J Photochem Photobiol B, Biol 2002;66:179–87. https://doi.org/10.1016/S1011-1344(02)00236-1.

[48] Chemeris YK, Shenderova LV, Venediktov PS, Rubin AB. Activation of chlororespiration increases chlorophyll fluorescence yield in Chlorella Adapted to darkness at high temperature. Biol Bull Russ Acad Sci 2004;31:143–50. https://doi.org/10.1023/B:BIBU.0000022469.13610.d7.

[49] Walker D. Photosynthetic induction phenomena and the light activation of ribulose diphosphate carboxylase. New Phytol 1973;72:209–35. https://doi.org/10.1111/j.1469-8137.1973.tb02027.x.
[50] Ting CS, Owens TG. Limitations of the pulse-modulated technique for measuring the fluorescence characteristics of algae. Plant Physiol 1992;100(1):367–73. https://doi.org/10.1104/pp.100.1.367.
[51] Nowicka B. Practical aspects of the measurements of non-photochemical chlorophyll fluorescence quenching in green microalgae Chlamydomonas reinhardtii using Open FluorCam. Physiol Plant 2020;168:617–29. https://doi.org/10.1111/ppl.13003.
[52] Anzecc AA, Environment NZ. Council C., agriculture, Australia RMCo, New Zealand C. Australian and New Zealand guidelines for fresh and marine water quality. 2000. p. 1–103.
[53] Guo J, Wilken S, Jimenez V, Choi CJ, Ansong C, Dannebaum R, et al. Specialized proteomic responses and an ancient photoprotection mechanism sustain marine green algal growth during phosphate limitation. Nat Microbiol 2018;3:781–90. https://doi.org/10.1038/s41564-018-0178-7.
[54] Abu-Ghosh S, Dubinsky Z, Iluz D. Acclimation of thermotolerant algae to light and temperature interaction1. J Phycol 2020;56:662–70. https://doi.org/10.1111/jpy.12964.
[55] White AJ, Critchley C. Rapid light curves: a new fluorescence method to assess the state of the photosynthetic apparatus. Photosynthesis Res 1999;59:63–72. https://doi.org/10.1023/A:1006188004189.